

Temperature Dependence of Impact Ionization Coefficients in 4H-SiC

Hiroki Niwa^{1, a*}, Jun Suda^{1, b} and Tsunenobu Kimoto^{1, c}

¹Department of Electronic Science and Engineering, Kyoto University

A1-303, Kyotodaigaku-katsura, Nishikyo, Kyoto 615-8510, JAPAN

^aniwa@semicon.kuee.kyoto-u.ac.jp, ^bsuda@kuee.kyoto-u.ac.jp, ^ckimoto@kuee.kyoto-u.ac.jp

Keywords: impact ionization coefficient, avalanche breakdown, photodiode, high temperature, device simulation, breakdown voltage.

Abstract. Impact ionization coefficients of 4H-SiC were measured at room temperature and at elevated temperatures up to 200°C. Photomultiplication measurement was done in two complementary photodiodes to measure the multiplication factors of holes (M_p) and electrons (M_n), and ionization coefficients were extracted. Calculated breakdown voltage using the obtained ionization coefficients showed good agreement with the measured values in this study, and also in other reported PiN diodes and MOSFETs. In high-temperature measurement, breakdown voltage exhibited a positive temperature coefficient and multiplication factors showed a negative temperature coefficient. Therefore, extracted ionization coefficient has decreased which can be explained by the increase of phonon scattering. The calculated temperature dependence of breakdown voltage agreed well with the measured values not only for the diodes in this study, but also in PiN diode in other literature.

Introduction

Impact ionization coefficients are important material properties which determine the breakdown voltage and safe-operating area of power devices. In 4H-SiC, several studies have been done to measure them. The first work was conducted by Konstantinov *et al.*, where photomultiplication characteristics were measured using a He-Cd laser ($\lambda=325$ nm) on p⁺n diodes [1]. At the same time, Raghunathan and Baliga has also reported the impact ionization coefficient of holes (β) by EBIC measurement on a Schottky barrier diode [2], although obtained coefficients were much lower than those of Konstantinov and others reported to date. In the work of Hatakeyama *et al.*, they have measured the photomultiplication characteristics by using an Ar⁺-laser ($\lambda=350$ nm) on p⁺n diodes on the Si-face and A-face of 4H-SiC, and showed the anisotropy of avalanche breakdown and impact ionization coefficients [3, 4]. For these studies, however, Loh *et al.* have pointed out a problem in the measurement procedures: the penetration depth of the illumination light (or electron beam) was too long and caused considerable carrier generation inside the depletion layer [5]. This caused an increase in mixed carrier injection and resulted in an error in multiplication factors. Recently, Green *et al.* has presented ionization coefficients derived from the photomultiplication and excess noise measurement using a frequency doubled Ar⁺ laser with a wavelength of 244 nm, and showed that electron ionization coefficient (α) exhibits strong electric field dependence at low electric field [6].

On the other hand, we have encountered a fact that calculation of breakdown voltage using Loh and Green's coefficients does not completely reproduce the experimental doping concentration dependence of breakdown voltage in other literatures. Since the reported ionization coefficients show clear variation to each other, accurate device simulation of breakdown voltage is still an open issue. Impact ionization coefficients need to be first determined at room temperature by taking account of the illumination wavelength as pointed out by Loh. Then a comparison of the calculated and measured breakdown voltages of a diode should be done. Furthermore, since one of the main benefits SiC power devices is high-temperature operation, values of impact ionization coefficients at elevated temperatures will be especially important. However, reports on high-temperature measurement of ionization coefficients are very limited in 4H-SiC [4, 7, 8]. Therefore, measurement is needed to accurately design and analyze high temperature operation SiC devices.

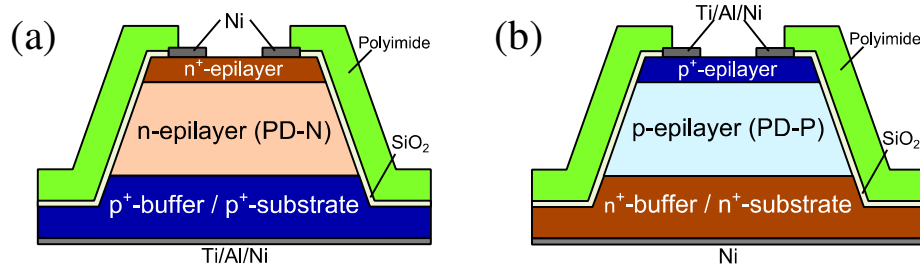


Fig. 1: Schematic cross section of the fabricated PDs. (a) n^+ - n - p^+ buffer / substrate (PD-N) (b) p^+ - p - n^+ buffer / substrate (PD-P). Structures of the layers are shown in Table 1.

In this study, impact ionization coefficients were measured by using two complementary p^+n and n^+p 4H-SiC photodiodes. Photomultiplication measurements were conducted at room temperature and elevated temperatures up to 200°C using a short-wavelength illumination source for accurate measurement of multiplication factors without mixed carrier injection. The extracted ionization coefficients were used to calculate breakdown voltage and comparison with the measured values were done for the PDs in this study and devices in literatures.

Table 1: Structures of the layers in PDs.

	PD-N	PD-P
n^+/p^+ epilayer	$N_d=1 \times 10^{19} \text{ cm}^{-3}$ 1 μm	$N_a=1 \times 10^{19} \text{ cm}^{-3}$ 1 μm
n/p epilayer	$N_d=4.0 \times 10^{16} \text{ cm}^{-3}$ 13 μm	$N_a=3.7 \times 10^{16} \text{ cm}^{-3}$ 12 μm
p^+/n^+ buffer	$N_a=2 \times 10^{18} \text{ cm}^{-3}$	$N_d=2 \times 10^{18} \text{ cm}^{-3}$

Device Fabrication and Measurement

Fig. 1 shows the schematic cross sections for the two types of fabricated PDs. Junction of PD-N (Fig. 1 (a)) consists of an n-type epilayer (13 μm , $N_d=4.0 \times 10^{16} \text{ cm}^{-3}$) grown on a p^+ -type buffer layer and substrate, and PD-P (Fig. 1 (b)) consists of a p-type epilayer (12 μm , $N_a=3.7 \times 10^{16} \text{ cm}^{-3}$) grown on an n^+ -type buffer layer and substrate. The precise structures of the layers are shown in Table 1. Here, both diodes do not punchthrough at the breakdown voltage. To avoid the electric field crowding, positive-bevel edge termination was employed by etching into the substrate using Cl_2 -based ICP-RIE with SiO_2 as an etching mask. After the deep mesa etching, 40-nm-thick oxides were formed for passivation by dry oxidation at 1300°C for 40 min, followed by nitridation in NO (10% diluted in N_2) at 1250°C for 70 min. Ti/Al/Ni and Ni annealed at 1000°C for 2 min were employed as ohmic contacts for the p^+ -type and n^+ -type, respectively. After the metallization, a 6- μm -thick polyimide was coated also as a passivation layer.

In the photomultiplication measurement, Xe-lamp combined with a band pass filter (BPF) of mainly 260 nm was used as an almost monochromatic illumination source. The penetration depth of the illuminated light with wavelength of 260 nm is 0.4 μm [9] so a pure carrier injection can be obtained since absorption in depletion layer is extremely small. The authors measured the optical transmission spectrum of a polyimide film, and confirmed the coated polyimide cuts off UV-light below 350 nm and will prevent the unwanted illumination to the mesa sidewalls or edges. In this study, three devices for each PD were measured, and all of the measured PDs had a diameter of 200 μm , free of macroscopic defects.

Results and Discussions

Measurement of Multiplication Factors. Fig. 2 shows the reverse I - V characteristics of (a) PD-N and (b) PD-P at various temperatures. Both of the diodes showed a positive temperature coefficient of breakdown voltage, indicating the avalanche breakdown. In the high-temperature measurement of the photocurrent, BPF was changed (260 nm \rightarrow 270, 280 nm) to obtain enough photocurrent, because the photocurrent decreased due to the increase of absorption coefficient at high temperature.

When calculating the multiplication factors, the initial unmultiplied current needs to be derived. Since the illuminated light is mainly absorbed near the surface of the diode, pure hole diffusion

current and pure electron diffusion current from the top n^+ and p^+ layers will be the main component of the photocurrent in PD-N and PD-P, respectively. Therefore, pure hole-initiated multiplication factor M_p can be measured from PD-N, and electron-initiated multiplication factor M_n can be measured from PD-P. The initial unmultiplied current can be obtained by fitting the equation of the diffusion current [10] to the measured photocurrent in the low reverse bias region where avalanche multiplication is not occurring. Then by dividing the measured current by the unmultiplied current, M_p and M_n were determined as shown in Fig. 3.

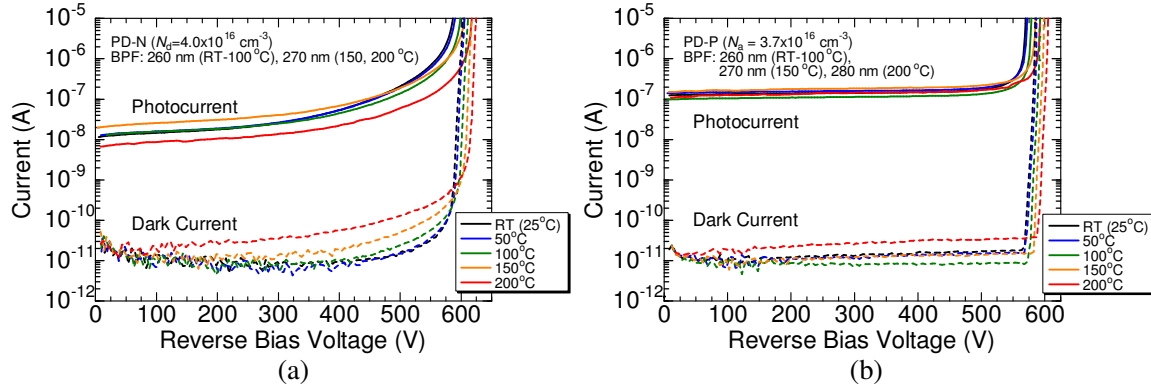


Fig. 2: Dark and photocurrent of the (a) PD-N and (b) PD-P at room temperature and up to 200°C.

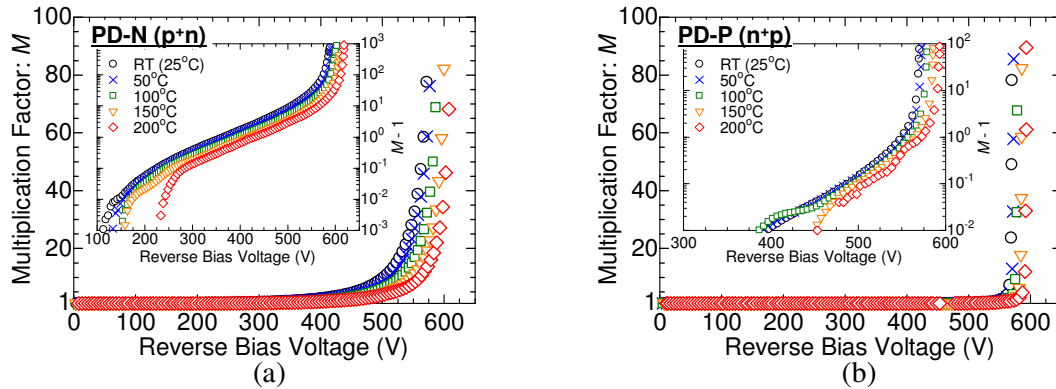


Fig. 3: Voltage dependence of multiplication factors. Inset shows the plot of $(M(V)-1)$ on a logarithmic scale. (a) PD-N: measurement of M_p . (b) PD-P: measurement of M_n .

From Fig. 3, it can be seen that M_p starts to increase at relatively low voltage, whereas M_n increases abruptly near the breakdown voltage. This indicates that the hole ionization coefficient β is considerably higher than the electron ionization coefficient α at low electric field, which agrees well with the previous results [1, 3, 5, 6]. As the temperature increases, both of the multiplication factors decrease resulting in the positive temperature coefficient of breakdown voltage. This measurement also indicates the negative temperature coefficient of β and α , as in the case of other semiconductor materials.

Extraction of Ionization Coefficients. When extracting ionization coefficients from multiplication factors, several methods have been proposed in various materials [11-13]. However, these methods use M_p and M_n obtained from measurement of a single device, and therefore these methods cannot be used in this study where M_p and M_n are obtained from separate complementary PDs. Thus, ionization coefficients were extracted using the following method. For the extraction of β , $\alpha \rightarrow 0$ or $M_n \rightarrow 1$ can be assumed at sufficiently low electric field, since it is known that β is much higher than α . Under this assumption, β can be expressed by converting the expression by Woods *et al.* as [11]:

$$\beta = \frac{qN_d}{\epsilon_0 \epsilon_s} \cdot \frac{1}{M_n' M_p} \cdot \frac{dM_p}{dE_m} \sim \frac{qN_d}{\epsilon_0 \epsilon_s} \cdot \frac{1}{M_p} \cdot \frac{dM_p}{dE_m} \quad (1)$$

Here, N_d is the doping concentration for the lightly doped layer of PD-N, and E_m is the electric field at the pn junction. M_n' is the electron multiplication factor measured from p^+n diode, and the measured

M_n obtained from n^+p diode in this study cannot be used. The calculated result of Eq. 1 is fitted using Chynoweth's expression [14]: $\alpha, \beta = a_{e,h} \exp(-b_{e,h}/E)$ at low electric field where the assumption $M_n \rightarrow 1$ stands valid. Here, E is the electric field and $a_{e,h}$ and $b_{e,h}$ are the fitting parameters. To extract α , by combining the ionization integrals of electrons and holes, the following equation can be derived.

$$\alpha = \frac{qN_a}{\epsilon_0 \epsilon_s} \cdot \frac{1}{M_n^2} \cdot \frac{dM_n}{dE_m} \cdot \left(\frac{qN_d}{\epsilon_0 \epsilon_s} \cdot \frac{1}{\beta M_p^2} \cdot \frac{dM_p}{dE_m} \right)^{\frac{N_d}{N_a}} \quad (2)$$

Here, N_d and N_a are the doping concentration for the lightly doped layer of PD-N and PD-P, respectively. Even though the doping concentrations of the two PDs are slightly different, α can still be accurately calculated.

Fig. 4 shows the obtained α and β , together with fitting results using Chynoweth's expression. The field dependence of ionization coefficients at room temperature can be expressed as follows.

$$\alpha = 8.19 \times 10^9 \cdot \exp\left(-\frac{3.94 \times 10^7}{E}\right) \quad [\text{cm}^{-1}] \quad (3)$$

$$\beta = 4.48 \times 10^6 \cdot \exp\left(-\frac{1.28 \times 10^7}{E}\right) \quad [\text{cm}^{-1}] \quad (4)$$

Compared with the previous results, β is taking a slightly higher value than that of Konstantinov. This may be due to the difference in the wavelength of the illumination source used in the measurement. For α , differences in β and the extraction method of α may be the reason for the difference, where direct calculation was used in this study and fitting procedure to the measured M_p was performed in the study of Konstantinov. However, as shown in Fig. 5 (a), the calculated breakdown voltage using the ionization coefficients obtained in this study agrees very well with the experimental values, indicating the successful extraction. Furthermore, calculated doping concentration dependence of breakdown voltage agrees fairly well with experimental results by Hatakeyama, too. Fig. 5 (b) shows the calculated results of the breakdown voltage of PiN structure with various i-layer thicknesses. In the figure, breakdown voltages of PiN diodes and MOSFETs from other literatures are also shown [15-18]. It can be seen that most of the calculated ideal breakdown voltages are close to the experimental values. From these results, the measured ionization coefficients in this study can be used for accurate design of a few kV-class devices.

Fig. 6 shows the extracted impact ionization coefficients at elevated temperatures. The result was also fitted using Chynoweth's expression. As it can be seen, the obtained β decreased as the

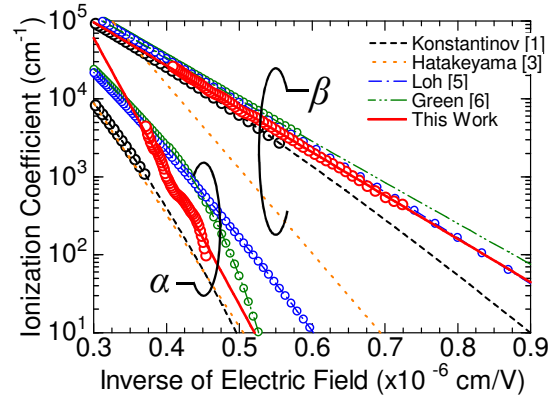


Fig. 4: The measured ionization coefficients (symbol) and the modeled data (lines) obtained at room temperature. Measurements of past literatures are also shown, where the symbols represent the range of the electric field where the measurement was done.

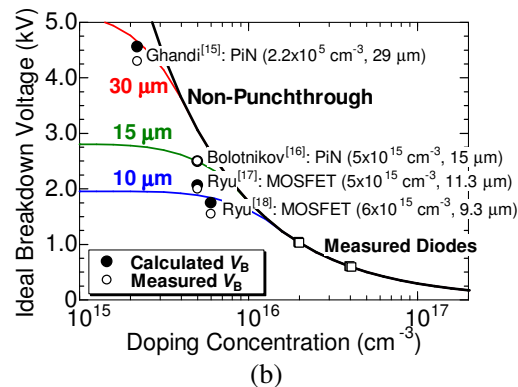
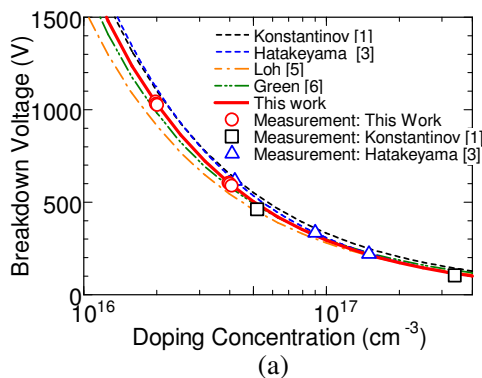


Fig. 5: Calculated doping concentration dependence of breakdown voltage for (a) p^+n non-punchthrough diodes at room temperature and (b) PiN structure with various i-layer thicknesses.

temperature increased. This temperature dependence of a_h and b_h in Chynoweth's expression can be described by the following equation where T is in Kelvin:

$$a_h = 3.94 \times 10^6 - 1.96 \times 10^4 \cdot T + 71.7 \cdot T^2 \text{ [cm}^{-1}\text{]} \quad (5)$$

$$b_h = 7.51 \times 10^6 + 1.77 \times 10^4 \cdot T \text{ [V/cm]} \quad (6)$$

These equations are valid at room temperature and at elevated temperatures up to 200°C. The negative temperature coefficient of β can be explained by the increase of phonon scattering [19]. This reduces the mean free path for the optical phonon generation, leading to the reduction of carrier energy obtained from the electric field. For future works, theoretical modeling should be made after measurement of ionization coefficients at lower electric field. For α , its temperature dependence was very small in the range of the measured electric field ($1/E < 0.4$ cm/MV) and could not be clearly measured. Therefore in this study, α at room temperature was used for the calculation of breakdown voltage at elevated temperature.

Fig. 7 (a) shows the calculated and measured temperature dependence of breakdown voltage. Dashed and solid lines denote the calculated results using Eq. 3, 5, and 6. Although the temperature dependence of α was not considered, calculation and measurement show good agreement to each other. Fig. 7 (b) shows the calculated and experimental breakdown voltages of a PiN diode reported by Mitlehner, where a blocking layer of $N_d = 8 \times 10^{15} \text{ cm}^{-3}$ and $w = 14 \text{ }\mu\text{m}$ was used [20]. Here, calculation of breakdown voltage using temperature dependence of ionization coefficients by Hatakeyama [4] and Loh [7] are also shown. The experimental values are slightly lower than the calculation, probably due to the electric field crowding, but the temperature dependence agrees well with the calculated result of our work.

Summary

The temperature dependence of impact ionization coefficients in 4H-SiC was measured. Two complementary 4H-SiC photodiodes were used for M_p and M_n measurements, and an original extraction method of ionization coefficients was presented. The obtained ionization coefficients at room temperature reproduce measured breakdown voltage very well for a few kV-class devices. From the high temperature measurement up to 200°C, a negative temperature coefficient of β was obtained. The temperature dependence of α was very small, and calculation of breakdown voltage using temperature dependence of β and α at room temperature agreed well with the experimental results. These results suggest the validness of the measured ionization coefficients for designing and analyzing a few kv-class 4H-SiC power devices.

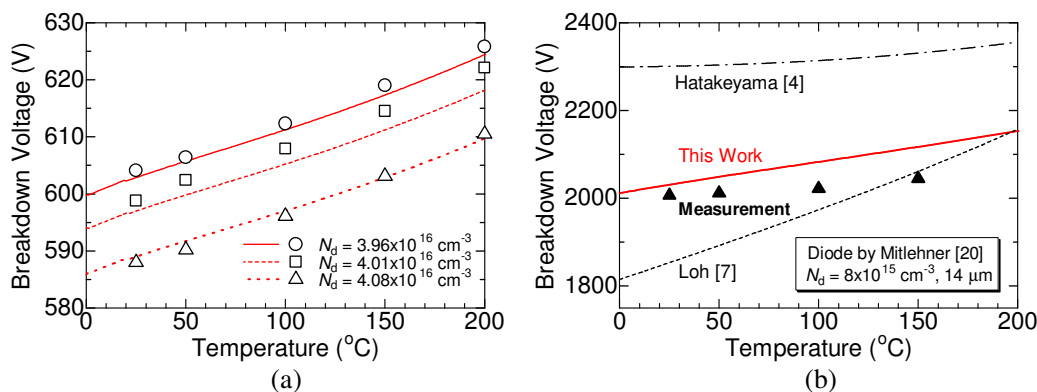


Fig. 7: Calculated and experimental temperature dependencies of breakdown voltage. (a) Diodes in this work, and (b) PiN diode by Mitlehner *et al.* [20]

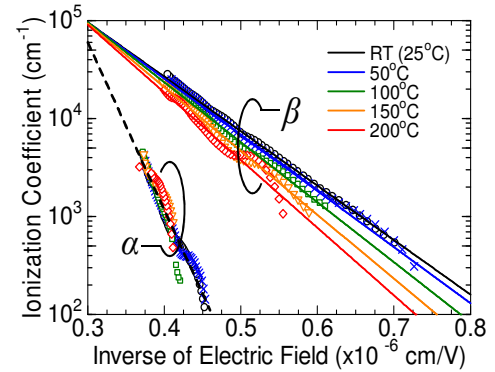


Fig. 6: The measured ionization coefficients (symbol) and the modeled data (lines) obtained at elevated temperatures up to 200°C.

Acknowledgement

This work was supported by the Funding Program for World-Leading Innovative R&D on Science and Technology (FIRST Program) and a Grant-in-Aid for Scientific Research (21226008) from the Japan Society for the Promotion of Science.

References

- [1] A. O. Konstantinov, Q. Wahab, N. Nordell, and U. Lindefelt, *Appl. Phys. Lett.*, vol. 71 (1997), p. 90.
- [2] R. Raghunathan and B. J. Baliga, *Proc. Int. Symp. Power Semicond. Devices ICs 1997*, p. 173.
- [3] T. Hatakeyama, T. Watanabe, T. Shinohe, K. Kojima, K. Aarai, and N. Sano, *Appl. Phys. Lett.*, vol. 85 (2004), p. 1380.
- [4] T. Hatakeyama, *Phys. Stat. Sol. (a)*, vol. 206 (2009), p.2284.
- [5] W. S. Loh, B. K. Ng, S. I. Soloviev, H.-Y. Cha, P. M. Sandvik, C. M. Johnson, and J. P. R. David, *IEEE Trans. Electron Devices*, vol. 55 (2008), p. 1984.
- [6] J. E. Green, W. S. Loh, A. R. J. Marshall, B. K. Ng, R. C. Tozer, J. P. R. David, S. I. Soloviev, and P. M. Sandvik, *IEEE Trans. Electron Devices*, vol. 59 (2012), p. 1030.
- [7] W. S. Loh, J. P. R. David, B. K. Ng, S. I. Soloviev, P. M. Sandvik, J. S. Ng, and C. M. Johnson, *Mater. Sci. Forum*, vol. 615-617 (2009), p. 311.
- [8] R. Raghunathan and B. J. Baliga, *Solid-State Electron.*, vol. 43 (1999), p. 199.
- [9] H.-Y. Ha and P. M. Sandvik, *Jpn. J. Appl. Phys.*, vol. 47 (2008), p.5423.
- [10] C. Raynaud, D.-M. Nguyen, N. Dheilily, D. Tournier, P. Brosselard, M. Lazar, and D. Planson, *Phys. Stat. Sol. (a)*, vol. 206 (2009), p. 2273.
- [11] M. H. Woods, W. C. Johnson, and M. A. Lampert, *Solid-State Electron.*, vol. 16 (1973), p. 381
- [12] W. N. Grant, *Solid-State Electron.*, vol. 16 (1973), p. 1189.
- [13] G. E. Bulman, L. W. Cook, and G. E. Stillman, *Solid-State Electron.* vol. 25 (1982), p. 1189.
- [14] A. G. Chynoweth, *Phys. Rev.*, vol. 109 (1958), p. 1057.
- [15] R. Ghandi, B. Buonno, M. Domeij, G. Malm, C.-M. Zetterling, and M. Östling, *IEEE Electron Device Lett.*, vol. 30 (2009), p. 1170.
- [16] A. V. Bolotnikov, P. G. Muzykov, Q. Zhang, A. K. Agarwal, and T. S. Sudarshan, *IEEE Trans. Electron Devices*, vol. 57 (2010), p. 1930.
- [17] S.-H. Ryu, S. Krishnaswami, M. Das, B. Hull, J. Richmond, B. Heath, A. Agarwal, J. Palmour, and J. Scofield, *Proc. Int. Symp. Power Semicond. Devices ICs 2005*, p. 275.
- [18] S.-H. Ryu, L. Cheng, S. Dhar, C. Capell, C. Jonas, R. Callanan, A. Agarwal, J. Palmour, A. Lelis, and C. Scozzie, *Proc. Int. Symp. Power Semicond. Devices ICs 2011*, p. 227.
- [19] C. R. Crowell and S. M. Sze, *Appl. Phys. Lett.*, vol. 9 (1960), p. 242.
- [20] H. Mitlehner, P. Friedrichs, D. Peters, R. Schörner, U. Weinert, B. Weis, and D. Stephani, *Proc. Int. Symp. Power Semicond. Devices ICs 1998*, p. 127.

Silicon Carbide and Related Materials 2013

10.4028/www.scientific.net/MSF.778-780

Temperature Dependence of Impact Ionization Coefficients in 4H-SiC

10.4028/www.scientific.net/MSF.778-780.461